INTERNATIONAL JOURNAL OF CLIMATOLOGY
Int. J. Climatol. **31**: 1309–1321 (2011)
Published online 2 June 2010 in Wiley Online Library
(wileyonlinelibrary.com) DOI: 10.1002/joc.2161

RMetS
Royal Meteorological Society

Regionality of monsoon onset in South America: a three-stage conceptual model

Rosana Nieto-Ferreira* and Thomas M. Rickenbach
Department of Geography, East Carolina University, Greenville, NC 27858-4353, USA

ABSTRACT: The evolution of monsoon onset across South America has complex temporal and regional variability that are controlled by local and remote land–ocean–atmosphere processes. In this study, a three-stage conceptual model for the onset of the South American monsoon season is proposed based on a rain threshold analysis and a rotated empirical orthogonal function (REOF) analysis of the Global Precipitation Climatology Project version 2 (GPCP-v2) dataset. This two-pronged approach allowed the identification of regions of South America that share a common seasonal cycle of rainfall variability and likely have a common mechanism for monsoon onset.

According to this model, the first stage of onset starts around pentad 59 (October 18–22) when precipitation begins in the northwestern part of the continent and gradually progresses towards the south and southeast. The second stage is marked by the abrupt establishment of the South Atlantic Convergence Zone (SACZ). This stage occurs on average around pentad 61 (October 28–November 1). The third stage of monsoon onset involves the late arrival of the monsoon to the mouth of the Amazon River, associated with the slow migration of the Atlantic Intertropical Convergence Zone (ITCZ). This final stage of onset occurs on average by pentad 73 (December 27–31). This three-stage model of onset provides a useful framework for the study of regional differences in monsoon onset mechanisms, a subject that is further explored in two companion studies. Copyright © 2010 Royal Meteorological Society

KEY WORDS South America; monsoon onset; evolution; regional

Received 11 November 2009; Revised 4 April 2010; Accepted 11 April 2010

1. Introduction

Monsoon precipitation has a profound influence on important interests in South America, including agriculture and hydroelectric power production (Rickenbach *et al*., 2009). These economic sectors stand to benefit from improved understanding of monsoon onset, and of how the pattern of onset changes from year-to-year. The goal of this study is to examine in detail the regional and temporal variability of South American Monsoon System (SAMS) onset across tropical and subtropical South America in order to improve our understanding of how SAMS onset evolves.

The seasonal cycle of precipitation in tropical South America shares general characteristics with classical monsoon climates in other parts of the world (Zhou and Lau, 1998) and is commonly referred to as the SAMS. The onset of the South American monsoon is complex and fundamentally associated with the seasonal migration of the Intertropical Convergence Zone (ITCZ) rainfall into the summer hemisphere. Figure 1 shows the annual cycle of rainfall averaged for 1998–2007 from the Global Precipitation Climatology Project version 2 (GPCP-v2, Adler *et al*., 2003). The South American monsoon region is highlighted by the dashed rectangle in Figure 1. During June–August almost no rain falls over the core of the Amazon region (region I). In September–October rainfall gradually spreads southeastward filling up the Amazon region. A springtime peak in mesoscale convective complex activity causes strong rainfall in region IV during October–November (Velasco and Fritsch, 1987). The South Atlantic Convergence Zone (SACZ, region III), identified as a southeastward extension of cloudiness from the Amazon Basin into the Atlantic Ocean, is quickly established in November. Rainfall comes to the mouth of the Amazon region (region II) only later, sometime in December–January. The South American monsoon gradually retreats between February and May. Hence climatologically, onset has been shown to begin over northwestern Brazil in September–October and to progress rapidly southeastward reaching southeastern Brazil by November–December, with onset delayed further along the northern coast of Brazil (Horel *et al*., 1989; Rao and Hada, 1990; Marengo *et al*., 2001; Zhou and Lau, 2001). An intriguing characteristic of the SAMS is its apparent rapid onset, which can take place within as little as a couple of weeks across parts of tropical and subtropical South America (e.g. Kousky, 1985; Horel *et al*., 1989; Gonzalez *et al*., 2007).

In the context of the SAMS, previous studies have defined monsoon onset based on precipitation, cloudiness, synoptic-scale flow fields or a combination of these

* Correspondence to: Rosana Nieto-Ferreira, East Carolina University, Greenville, NC 27858-4353, USA. E-mail: ferreirar@ecu.edu

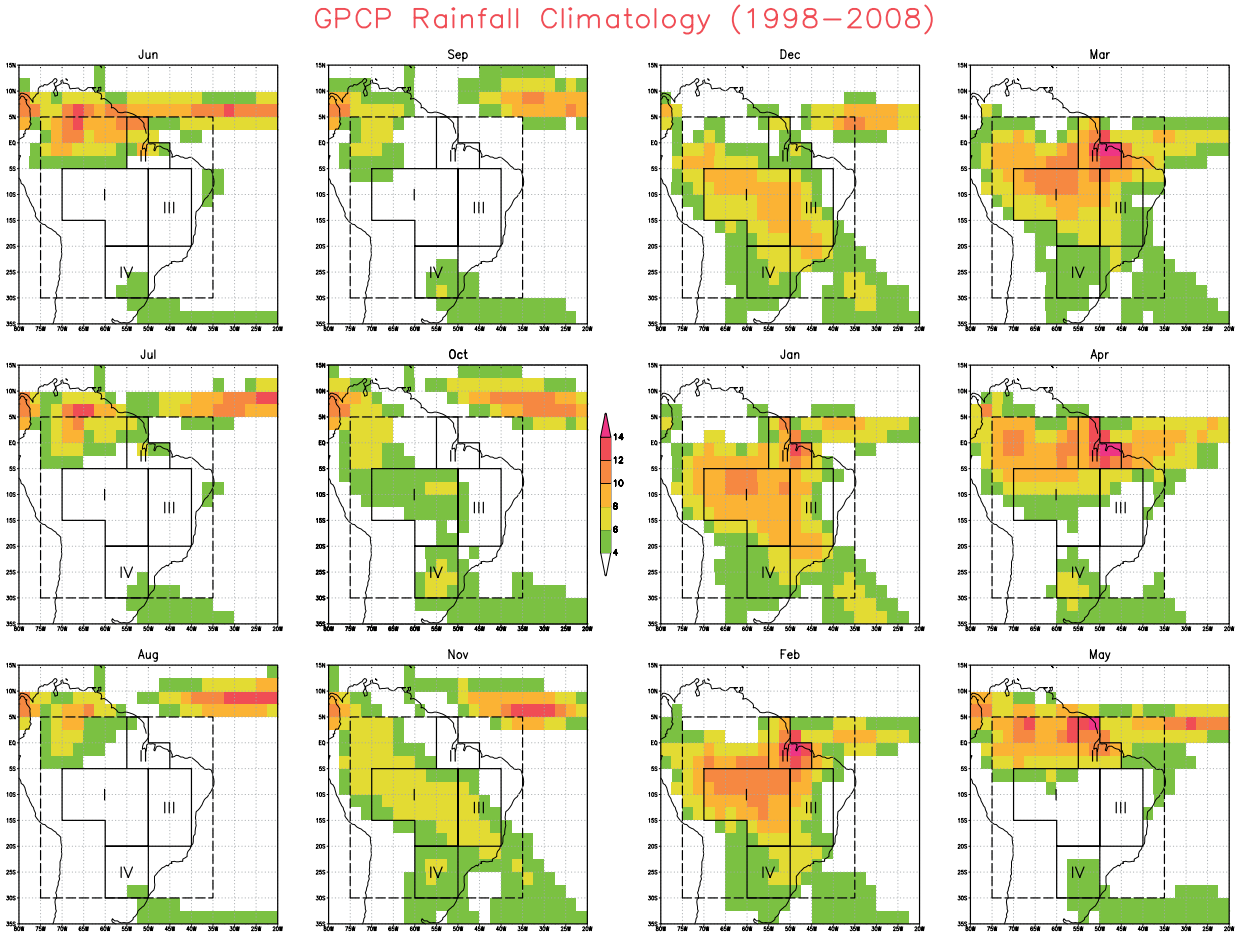

Figure 1. Mean annual cycle of precipitation in South America from the GPCP precipitation dataset (1979–2008). Dashed box shows the SAMS region studied in this paper. Solid boxes represent the regions where the three main modes of variability captured by the REOF analysis have strong influence, namely region I corresponds to REOF1, region II corresponds to REOF2 and regions III and IV correspond to the two sides of the dipole captured by REOF3. This figure is available in colour online at wileyonlinelibrary.com/journal/joc

(e.g. Gandu and Geisler 1991; Lenters and Cook, 1995; Liebmann *et al*., 1999; Fu and Li, 2004; Li and Fu, 2004; Machado *et al*., 2004; Li and Fu, 2006). Some studies have defined onset date as the time when sustained wet season cloudiness (Kousky, 1988; Horel *et al*., 1989; Garcia and Kayano, 2009) or precipitation (Liebmann and Marengo, 2001; Marengo *et al*., 2001; Li and Fu, 2006) above the seasonal mean begins in a particular region. The Outgoing Longwave Radiation (OLR) studies of Kousky (1988) and Horel *et al*. (1989) indicated a general migration of low OLR values (proxy for convection) from the northwestern Amazon Basin to the southeast during September and October. By early November, convection covered the southern Amazon region indicating the general onset of the monsoon across the Amazon Basin. Marengo *et al*. (2001) used rain gauge data interpolated to a 2.5° grid across a portion of the SAMS region and found a similar pattern of onset. They used the mean annual rainfall across the Amazon Basin (4 mm day^{-1}) as a threshold and required that six of eight subsequent rainfall pentads remain 0.5 mm day^{-1} above the threshold, with six of eight prior rainfall pentads remaining 0.5 mm day^{-1} below the threshold. They found that the pattern of onset was very sensitive to this threshold value. Using a similar rainfall dataset, Liebmann and Marengo (2001) determined onset using different threshold values for each 2.5° grid box based on the climatological mean rainfall at each box. However, this technique yielded a reversed pattern of onset, starting in the southeast and migrating northwestward. Li and Fu (2004) used the mean climatological rainfall for the southern Amazon Basin region as the threshold value to study monsoon onset in the European Center for Medium Range Weather Forecasts (ECMWF) reanalysis data (ERA). Gonzalez *et al*. (2007) used the Kousky (1988) OLR technique over the entire SAMS region to study onset date. The average onset date from the OLR method was pentad 56 (Table I), or about seven pentads earlier than from ERA data, and about three pentads earlier than the rain gauge study (Marengo *et al*., 2001). The interannual variability of onset dates from the different methods are not generally consistent.

Other studies have taken an integrated approach to defining monsoon onset by creating indices based on low-level winds and precipitation (Gan *et al*., 2004, 2005), on the vertically integrated moisture transport by the zonal wind (Raia and Cavalcanti, 2008) in Amazonia,

Table I. Comparison of average onset pentad from various studies as follows: average onset pentad in regions I, II and III calculated in Section 3.1 using the rainfall threshold method (Figure 4(a), 1979–2008); average onset pentad in regions I, II and III calculated in Section 5 using the average PC1, PC2 and PC3 time series (Figure 9, 1979–2008); average onset pentad calculated using the ERA model rainfall by Li and Fu (2004, LF2004) over southern Amazonia (5–15 °S, 45–75 °W); average onset pentad (1979–2005) based on a combined EOF analysis by Silva and Carvalho (2007, SC2007) and Gan *et al*. (2004, GKR2004) average onset pentad (1979–1999) using the Kousky (1988) OLR onset method over central western Brazil (10–20 °S, 50–60 °W).

	Region I	PC1	LF2004	SC2007	GKR2004	Region II	PC2	Region III	PC3
Onset pentad	60	59	63	61	56	69	73	64	61

or on the northerly reversal of the low-level cross-equatorial flow (Wang and Fu, 2002; Li and Fu, 2004). Silva and Carvalho (2007) used a combined empirical orthogonal function (EOF) analysis of precipitation and various thermodynamic and dynamic low-level fields to obtain a large-scale index that describes intraseasonal-to-interannual variability of the South American monsoon and calculated that on average SAMS onset occurred on pentad 61 (Table I). Although there is some consistency between these studies on the average date and pattern of progression of monsoon onset in South America, they are not generally consistent in terms of interannual variability of onset dates and are in general limited to the Amazon Basin.

Against the backdrop of the slow southward shift in the ITCZ that drives the monsoon, regional variation in the timing and mechanisms of monsoon onset occur because of variations in topography, land surface characteristics, sea surface temperatures (SSTs), geography, and local and remote atmospheric phenomena. Driven by the southward migration of the sun, the gradual increase in sensible and latent heat fluxes, surface wetness and thermodynamic instability prime the atmosphere for convection during the pre-monsoon season (Li and Fu, 2006). However, each year the precise timing of monsoon onset is influenced by factors acting over a range of timescales from daily to interannual. For instance, during strong El Niño years, rainfall is generally suppressed over tropical South America because of enhanced large-scale subsidence in the Walker circulation over the Amazon. At the same time, onset is delayed in strong El Niño years in parts of the Amazon Basin (Marengo *et al*., 2001; Gan *et al*., 2004), though the mechanism for onset delay is not clear. Another remote factor that likely influences monsoon onset over South America is the seasonal variability of SSTs in the tropical Atlantic. During the austral winter and early spring, a cold tongue dominates the equatorial Atlantic and the warmest SSTs are located in the northern tropical Atlantic (e.g. Mitchell and Wallace, 1992). Since the oceanic ITCZ tends to be located over the warmest SSTs (e.g. Lindzen and Nigam, 1987) during austral winter and early austral spring the Atlantic ITCZ is located in the Northern Hemisphere. As the cold tongue weakens in the late austral spring and summer, the tropical Atlantic slowly transitions to a warm phase that peaks in March–April and the Atlantic ITCZ slowly migrates into the Southern Hemisphere (e.g. Mitchell and Wallace, 1992). Observational and modelling studies have shown that the seasonal march of convection over tropical South America in the 60–40 °W latitude band is dominated by the slow seasonal migration of the Atlantic SSTs and ITCZ (e.g. Hastenrath and Lamb, 1977; Rao and Hada, 1990; Mitchell and Wallace, 1992; Biasutti *et al*., 2004). It is hypothesized here that the late monsoon onset in tropical eastern South America observed in previous studies (e. g. Kousky, 1988; Marengo *et al*., 2001) is associated with the influence of the slow southward migrating Atlantic oceanic ITCZ as suggested by Figure 1.

Over South America, the timescale of alternating wet and dry phases in subtropical rainfall from Argentina to southeastern Brazil suggests that monsoon rain variability is linked to the Madden-Julian Oscillation (MJO, Nogues-Paegle and Mo, 1997; Jones and Carvalho, 2002; Gan and Moscati, 2003). Despite the lack of a clear connection between MJO and monsoon onset, Raia and Cavalcanti (2008) found that a low-frequency (MJO timescale) upstream blocking pattern in the upper-level winds occurs preferentially when onset is later than normal.

On yet shorter timescales, cold fronts associated with mid-latitude baroclinic systems can move far northward along the east side of the Andes Mountains and influence precipitation in tropical South America (Fortune and Kousky, 1983; Garreaud, 2000; Vera and Vigliarolo, 2000). In southeast Asia for example, frontal systems are recognized to play an important role in monsoon onset over the South China Sea (Chang and Chen, 1995) as warm moist southwesterly flow produce widespread rain along cold fronts that become stationary (termed the Baiyu or Mei-yu front). Cold fronts may play a similar role in SAMS onset. Li and Fu (2006) proposed that in South America, cold fronts may help trigger monsoon onset by enhancing forced ascent in a thermodynamically primed atmosphere. Raia and Cavalcanti (2008) found that the enhanced northwesterly moisture flux in central and southeast Brazil produced by cold fronts is also essential to SAMS onset. Why certain frontal systems might trigger onset along the SACZ axis and whether onset in the deep tropics is influenced by frontal systems remain important outstanding issues. A dynamical framework for the sudden onset of the SACZ is provided in Nieto-Ferreira and Rickenbach (2010). They

found that at the time of monsoon onset in the SACZ region, a sudden change in the behavior of cold fronts occurs with cold fronts not only suddenly becoming stationary in the SACZ region but also organizing a northwest–southeast oriented stationary band of convection that extends deep into the Amazon Basin. Their results suggest that increased anticyclonic shear on the equatorward side of the upper-level jet can trigger a regime change in the lifecycles of mid-latitude baroclinic waves (e.g. Thorncroft *et al*., 1993). The increased anticyclonic shear favours the formation of 'thinning' upper-level troughs that intrude farther into lower latitudes and become elongated in the northwest–southeast direction, sometimes producing cut-off cyclones that wander into the tropics. The surface signature of such 'thinning' upper-level troughs is characterized by long fronts that extend into the tropics and propagate very slowly (e.g. Thorncroft *et al*., 1993), precisely the characteristics associated with the cold fronts associated with monsoon onset in the SACZ region in the Nieto-Ferreira and Rickenbach (2010) composites.

This study builds on previous studies of monsoon onset definition, timing and regional variability to construct an integrated picture of monsoon onset and to propose a three-stage conceptual model of monsoon onset in South America. This model serves as a basis for detailed studies of regional onset mechanisms (e.g. Nieto-Ferreira and Rickenbach, 2010). This paper is organized as follows. Section 2 discusses the datasets used in this study. Section 3 studies the local variability of monsoon onset in the GPCP v2 dataset using a rainfall threshold-based monsoon onset analysis over $5^\circ \times 5^\circ$ boxes in tropical and subtropical South America. The interannual variability of monsoon onset is also analyzed in this section. Section 4 studies differences in the evolution of monsoon onset in the eastern and western domains of the SAMS. Section 5 uses a rotated empirical orthogonal function (REOF) analysis of pentad averaged GPCP rainfall to discuss regional patterns of monsoon onset. The results of the analyses above are then integrated to construct a three-stage conceptual model of SAMS onset. Conclusions and future work are discussed in Section 6.

2. Datasets

Although regional SAMS onset dates have been previously estimated using rain gauge or reanalysis data for portions of our domain and period of interest (Marengo *et al*., 2001; Li and Fu, 2006), in this study we calculate onset dates using a homogeneous criterion and a uniform dataset over the entire SAMS domain. The GPCP-v2 precipitation dataset (Adler *et al*., 2003) is used to determine SAMS onset across tropical and subtropical South America from 1979 to 2007. The GPCP-v2 2.5° pentad precipitation dataset provides rainfall estimates using an optimization of satellite and gauge data. The strength of the GPCP-v2 product is that it is uniform in time and space, covers all of South America and is tuned to the more physically direct precipitation retrieval of microwave satellites, including the Tropical Rainfall Measuring Mission (TRMM) satellite. TRMM observations of the horizontal organization and internal structure of convective systems prior to and following SAMS onset will be presented in a subsequent study in preparation. Details of the production of the GPCP-v2 dataset are described in Adler *et al*. (2003). The combination of homogeneous temporal and spatial resolutions on daily-to-interannual timescales over the global tropics makes the GPCP-v2 a very well-suited dataset for monsoon studies.

An important reason for using a standardized satellite-based precipitation dataset (the GPCP-v2) is that previous studies of SAMS onset are not in general agreement regarding the timing and pattern of onset across South America. In these studies, different data were used to characterize onset such as satellite OLR (Kousky, 1988; Horel *et al*., 1989), surface rain gauge networks of limited spatial and temporal coverage (Liebmann and Marengo, 2001; Marengo *et al*., 2001), or ECMWF reanalysis model precipitation (Li and Fu, 2004).

The approach used in this study is two-pronged. First, the onset date for each year is determined in $5^\circ \times 5^\circ$ boxes over land using an objective criterion that identified sustained rainfall above the climatological mean (based on Marengo *et al*., 2001). Next an REOF analysis is performed on the GPCP-v2 data to help identify regions of South America that share a similar seasonal cycle of rainfall variability and likely a common onset mechanism. Results from these two approaches are contrasted and integrated to develop a conceptual model of SAMS onset.

3. Local monsoon onset: rainfall threshold analysis

In this section, a rainfall threshold monsoon onset definition is used to calculate a local onset date for every $5^\circ \times 5^\circ$ box across the SAMS. This approach allows us to not only study the progression of monsoon onset across the SAMS but also allows us to compare our results to those of previous studies.

The 1979–2007 mean GPCP-v2 precipitation climatology is shown in Figure 2. GPCP-v2 captures well-known features of the climatology including maxima of 8–10 mm day^{-1} near the equator in western Amazonia and at the mouth of the Amazon River, as well as a minimum in northeast Brazil. A relatively weaker maximum of precipitation (4–6 mm day^{-1}) occurs in southern Brazil and Uruguay because of the presence of frontal systems and large mesoscale convective complexes (e.g. Velasco and Fritsch, 1987). In Figure 2, the SACZ is evident as a swath of precipitation extending southeastward from the Amazon Basin into the South Atlantic Ocean. In this study, we focus on the entire SAMS region, defined here by the area enclosed by 5°N–30°S, 75–35°W (dashed region of Figure 2). The mean rain rate for 1979–2007 in the SAMS region as a whole from GPCP-v2 was 4.6 mm day^{-1}.

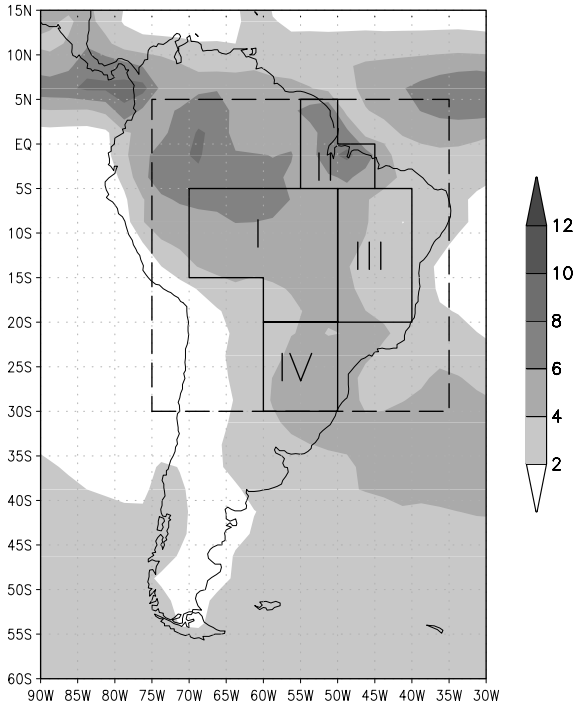

Figure 2. The 1979–2007 GPCP-v2 precipitation climatology (mm day^{-1}) for South America from the 2.5° pentad data. Dashed box shows the SAMS region studied in this paper. Solid boxes represent the regions where the three main modes of variability captured by the REOF analysis have strong influence, namely region I corresponds to REOF1, region II corresponds to REOF2 and regions III and IV correspond to the two sides of the dipole captured by REOF3.

For the determination of monsoon onset dates, the GPCP-v2 pentad precipitation was averaged in $5^\circ \times 5^\circ$ boxes. This spatial averaging was performed in order to smooth the rain time series to ease identification of onset, and to be consistent with the spatial and temporal resolution of TRMM observations of convective structure in a subsequent study. The SAMS region (5°N–30°S, 75–35°W) was divided into 56 boxes each $5^\circ \times 5^\circ$ in size (Figure 3). In order to focus on the monsoon over land, boxes with half or more of the area covered by ocean were not used in the analysis. Time series of the GPCP-v2 pentad rainfall for each box were constructed for all years. The constant threshold technique of Marengo *et al*. (2001) was used with the following minor modifications. A constant onset threshold of 4.6 mm day^{-1} was used, which is the mean 1979–2007 GPCP-v2 rainrate within the SAMS onset area. For each year at each 5° box, if six of eight future pentads are at least 0.5 mm day^{-1} greater than the threshold and six of eight prior pentads are at least 0.5 mm day^{-1} less than the threshold, the current pentad is the onset date. When the six of eight future criteria is not strictly met, but future pentad rain oscillates with peak values twice the threshold for at least three of eight future pentads, the current pentad is the onset date. This last criterion was added to account for the variable active/break rain pattern present during the monsoon season, prevalent, for example, in southwestern Amazonia (Rickenbach *et al*., 2002).

The algorithm identified the monsoon onset pentad in each 5° box over land for each year between June of year n and June of year $n+1$, in order to capture the advance of the Southern Hemisphere monsoon. For that period, Southern Hemisphere onset precedes Northern Hemisphere onset as the ITCZ advances southward then retreats northward. For some boxes onset is clearly defined, while in others onset might not take place in a given year either because rain oscillates around the climatological mean threshold year-round, or because rain never exceeds the climatological mean threshold.

To illustrate variation in onset characteristics with location, the annual rainfall time series for five different 5° boxes for 1984 is shown in Figure 4. That year, onset was most clearly defined in central Amazonia (Box 19, early October, pentad 55) and for south-central Amazonia (Box 36, mid-October, pentad 57). In the dry northeast, onset was delayed to late February (Box 24, pentad 11). Onset was not defined in northwestern Amazon (Box 9), where it rains year-round. Note that in the southernmost region (Box 46), rainfall is highly variable because of transient frontal systems.

Once the onset pentad was determined for each year (June of year n to June of year $n+1$), the mean onset pentad for 1979–2007 at each box was calculated. This was done by averaging the onset pentad over all years at each box, while carefully accounting for the change in sequential pentad numbers from pentad 73 to pentad 1 (December to January transition) in determining the average.

3.1. Regional variability of onset

The mean onset pentad numbers for each box are shown in Figure 5(a), with darker shading indicating later onset. At the earliest stage of onset, the general pattern in the Southern Hemisphere tropics shows onset progressing from the northwest SAMS region (between 0–5°S) starting at pentad 54 (late September) and advancing southeastward to 20°S. In parts of the subtropics (region IV from Figure 1), onset begins slightly earlier at pentads 52 and 53 (mid-September) and spreads northward. Therefore, onset actually begins in the subtropics progressing northward, while about a pentad later in the tropics onset starts in the northwest progressing southeastward. The two onset patterns appear to converge at 15–20°S by pentads 61–62 (late October–early November). The southeastward progression of onset is well known, associated with the southward migration of the ITCZ. The northward onset progression in the subtropics is noteworthy, as it is likely related to the establishment of the SACZ as will be discussed later. After early November, onset broadens with time to the east and west from the main NW–SE axis of rainfall. In the southwestern subtropical SAMS region, onset is established by mid December (pentads 68, 69).

Along the mouth of the Amazon (boxes 13 and 14), onset occurs in early-to-mid December (pentads 67–69).

Figure 3. Network of 56 5° × 5° boxes covering the SAMS region between 5°N–30 °S latitude, 75–35 °W longitude. Monsoon onset was determined in each land box, identified with large bold numbers. Also shown is topographic elevation (metres). This figure is available in colour online at wileyonlinelibrary.com/journal/joc

In the drier Nordeste region (boxes 23 and 24), onset arrives in late December, and as late as the end of January (pentad 7) in the extreme eastern Nordeste region. In those regions, the Atlantic ITCZ is the dominant regulator of precipitation (Moura and Shukla, 1981; Mitchell and Wallace, 1992; Hastenrath and Greischar, 1993; Liebmann *et al*., 1999; Biasutti *et al*., 2004). The Atlantic ITCZ follows the seasonal migration of warm SSTs thus migrating much more slowly towards the south than the wet season rainfall over land. Thus by the end of December, the Southern Hemisphere monsoon is usually established across the SAMS region (except for the extreme eastern Nordeste region). North of the equator, onset occurs between late February and late March (pentads 12–19) as the ITCZ begins its northward march.

The frequency that onset criteria were met in each box between 1979 and 2007 is now discussed. Shown in Figure 5(b) is the percentage of years when the onset criteria is met. From the central SAMS region to the southeast coast of Brazil, within the main axis of monsoon rain, onset occurs every year. There are three general regions where onset does not consistently occur most years. First, in the northwest region just south of the equator (in agreement with Marengo *et al*., 2001), where mean onset begins and progresses to the southeast, onset occurs in only 10% of the years. This is because it rains year-round most years (e.g. Figure 4(a)). Second, in the southern subtropical region (south of 20 °S), where mean onset propagates northward, onset is not usually defined every year. Frontal systems bring periodic rain to this region even during wintertime, and during years when front are more active the onset criteria are not met. It is interesting that onset begins in the two regions where onset does not consistently occur each year, because of significant winter rainfall. Lastly, in the dry Nordeste region onset occurs in only about one-third of the years, because rainfall in this region does not generally reach the onset threshold.

3.2. Interannual variability of onset

The interannual variability of onset dates (for the years onset occurred) can be represented by the standard deviation (s.d.) of onset pentads in each 5° box (Figure 5(c)).

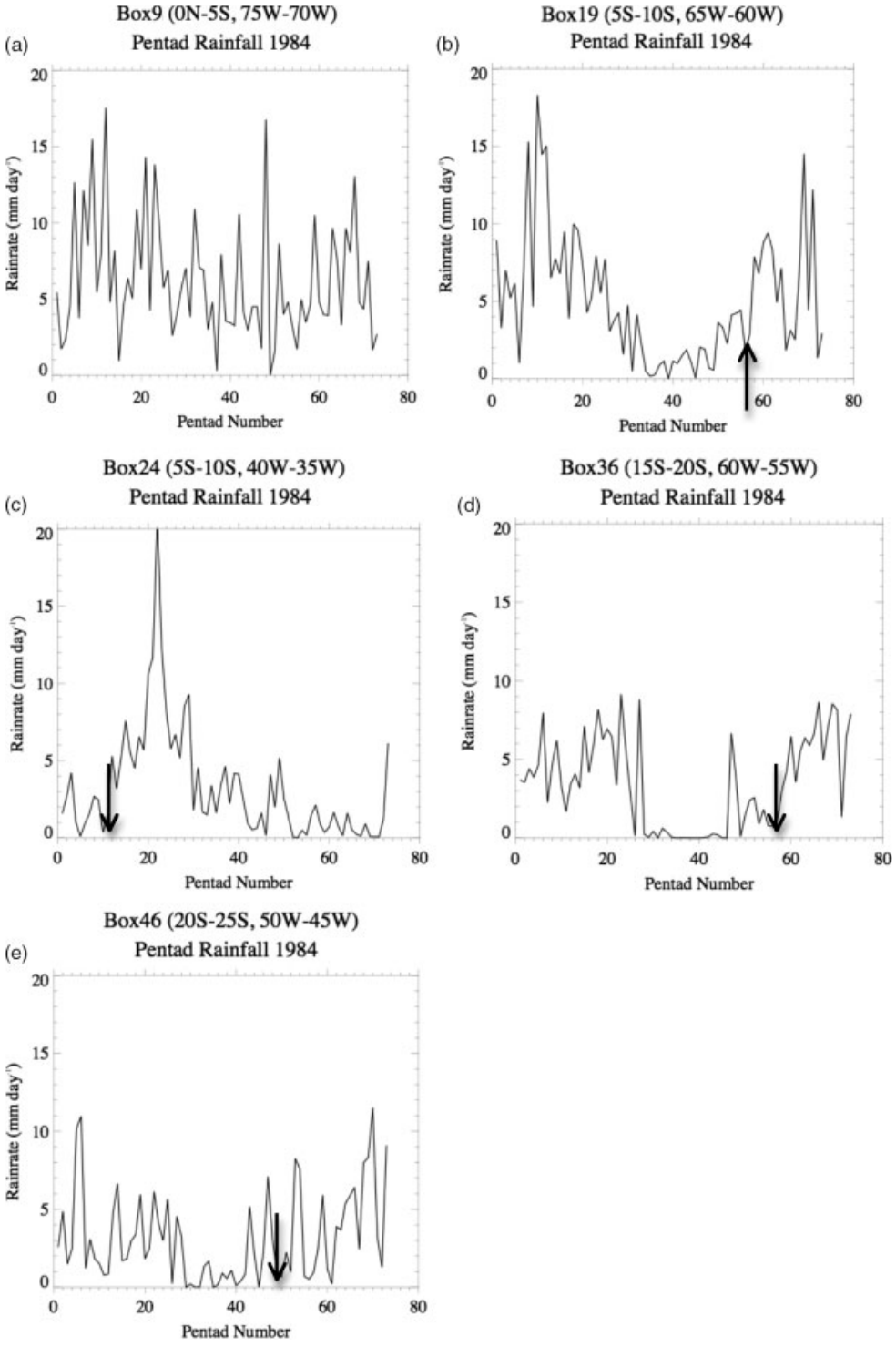

Figure 4. Time series of GPCP-v2 precipitation for five different 5° boxes in 1984, to illustrate onset characteristics of different regions. (a) Northwest Amazon (no onset); (b) central Amazon (onset pentad 55); (c) northeast Brazil (onset pentad 11); (d) south-central Amazon (onset pentad 57); (e) southeast Brazil (onset pentad 50).

The largest interannual variability of onset dates (highest s.d. values) occurs in the northwest SAMS region just south of the equator, where onset generally occurs less frequently due to year-round rainfall. However, in that region, large onset pentad variability (s.d. >6, or about 1 month) also occurs in boxes where onset occurs most of the years (Figure 5(b)). For example, for box 11 (at 0–5 °S; 65–60 °W), onset occurs in 60% of the years and is highly variable (s.d. = 9.7, or about 7 weeks). At the nearby box 17 (5–10 °S; 75–70 °W), onset occurs in 92% of the years while onset date variability is still large (s.d. = 6.0). In the central SAMS region, where onset occurs every year, onset date variability is lower ($3 <$ s.d. < 5). In the southeastern subtropics, onset date variability is often greater than 3–4 weeks (s.d. >5), again possibly connected to

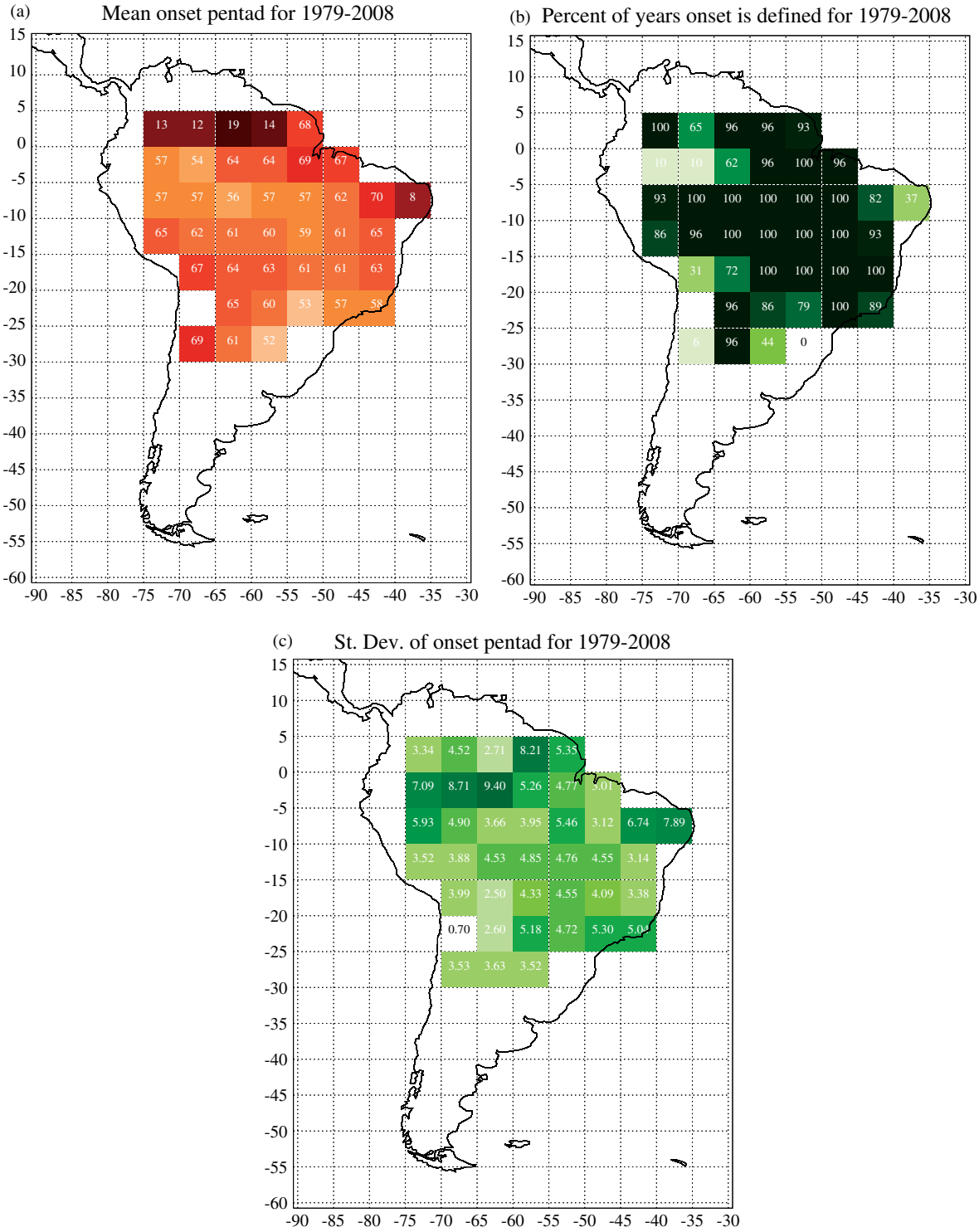

Figure 5. Mean onset statistics for 1979–2007 over the SAMS region. (a) Mean 1979–2007 onset pentads. Darker shading means later onset. Onset is defined starting in June of a given year. The blank land box at 25–30 °S, 55–50 °W has no pentad number because the onset criterion was never met there. (b) Percentage of years when onset occurs. Darker shading means onset occurs in more years. (c) Standard deviation (s.d.) of onset pentad for years when onset occurs. Darker shading means larger interannual variability (higher s.d.) in onset dates. This figure is available in colour online at wileyonlinelibrary.com/journal/joc

variability introduced by fronts. This means that the highest onset date variability in the SAMS domain occurs in the regions where SAMS onset begins, that is, the northwestern SAMS region and the southeastern subtropics. The Nordeste region of Brazil also has large onset date variability (of over a month), albeit with lower frequency of onset. Previous studies have found that the interannual variability of rainfall in northeast Brazil follows the interannual variability of Atlantic SSTs (e.g. Moura and Shukla, 1981).

Marengo *et al.* (2001) observed that in central Amazonia (a 4° radius circle centred at 5 °S, 59 °W) and at the

mouth of the Amazon River monsoon (a 3.5° radius circle centred at 0 °S, 49 °W) onset occurred later than usual during the 1982 and 1991 El Niño years and earlier than usual during the 1998 La Niña episode. The effect of the El Niño-Southern Oscillation (ENSO) on monsoon onset date variability is now revisited using a longer time series over the entire SAMS region. Figure 6 shows the average monsoon onset dates for El Niño and La Niña events that occurred between 1979 and 2006. During El Niño events, Figure 6(a) shows that monsoon onset dates are one-to-five pentads later than average over most of the SAMS region. The largest monsoon onset delays occur in the portion of the SAMS region between 0 and 10 °S. During the strong El Niño events of 1982 and 1997 (not shown), the delay in monsoon onset is longer reaching eight pentads later than average in parts of Amazonia. On the other hand, during La Niña episodes (Figure 6(b)) while there is a tendency for early monsoon onset dates in the 5°N–5 °S portion of the SAMS domain, there is a mix of early and late monsoon onset dates elsewhere in the SAMS domain. In good agreement with the results of Marengo *et al.* (2001) our results show that both at the mouth of the Amazon River (a 3.5° radius circle centred at 0 °S, 49 °W) and in central Amazonia (a 4° radius circle centred at 5 °S, 59 °W) monsoon onset is delayed during El Niño years and early during La Niña years. This is also in good agreement with the delay in monsoon onset over west-central Brazil during El Niño years found in Gan *et al.* (2004).

Other remote effects on the interannual variability of rainfall in the Amazon region are related to the interannual variability of Atlantic SSTs. For instance, during 2005 the Amazon region was affected by a strong drought that was most severe during the dry season (Zeng *et al.*, 2008). The meteorological component of this drought has been attributed to warm SSTs in the subtropical North Atlantic Ocean (Zeng *et al.*, 2008). Analysis of the time series for PC1 in 2005 shows that the 2005 dry season begun in the second week of April or about three pentads earlier than usual and ended on time. This means that the 2005 dry season in the Amazon Basin lasted about three pentads longer than usual. It is possible that the early start of the dry season in 2005 contributed to the rainfall deficits observed in April–June 2005.

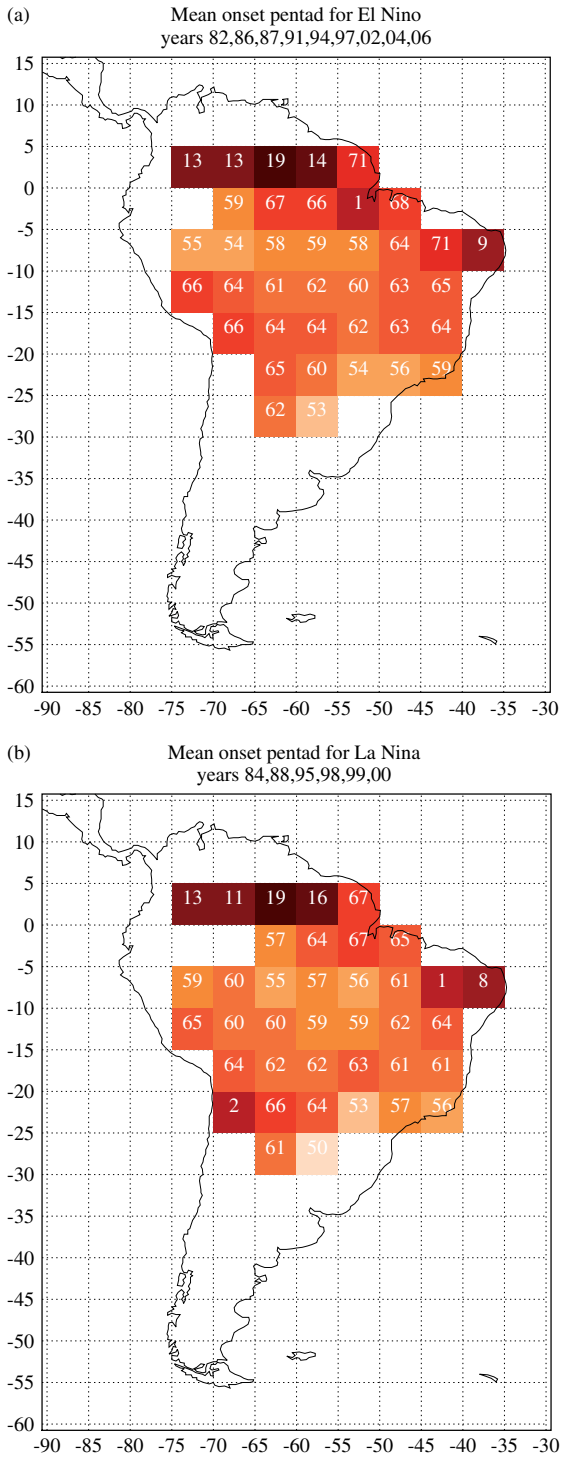

Figure 6. Mean SAMS onset pentad for (a) El Niño years (1982, 1986, 1987, 1991, 1994, 1997, 2002, 2004, 2006) and (b) La Niña years (1984, 1988, 1995, 1998, 1999, 2000). This figure is available in colour online at wileyonlinelibrary.com/journal/joc

4. SAMS west vs. east seasonal evolution of precipitation

The spatial pattern of onset pentads (Figure 5(a)) provides the context for results presented in the next sections. Figure 5(a) suggests that in addition to the monsoon progressing from northwest Amazonia to the southeastern coast of Brazil, onset also begins in subtropical South America and progresses northward. Figure 5(a) also shows that onset is delayed near the mouth of the Amazon River, and especially in northeastern Brazil.

Time-latitude plots of the 1979–2007 monthly mean GPCP-v2 rainfall for different sectors across the longitudinal span of South America are used to analyze the seasonal migration of precipitation in order to shed light on different regional mechanisms at play in SAMS onset. Figure 7(a) shows the seasonal migration of precipitation over the entire longitudinal span of the SAMS

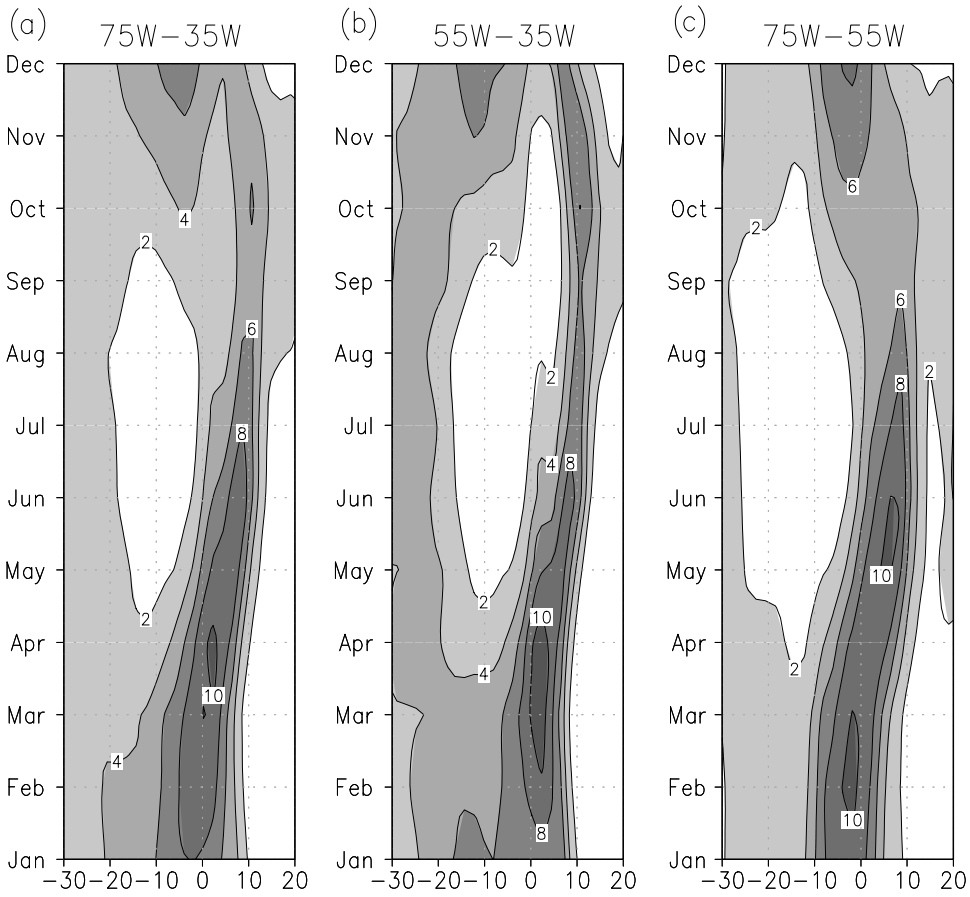

Figure 7. Time-latitude diagrams of the climatology GPCP-v2 rainfall averaged over the (a) SAMS region 75–35 °W, (b) west SAMS (75–55 °W) and (c) east SAMS (55–35 °W).

(75–35 °W) and shows that while the migration of the precipitation from the Southern Hemisphere to the Northern Hemisphere during the austral fall occurs gradually between April and June, the migration of the precipitation back to the Southern Hemisphere in the austral spring follows a more complicated pattern. Sometime in October, precipitation quickly begins near 10 °S while in the Northern Hemisphere precipitation lingers on near 5–10°N until December. In order to study in more detail the migration of precipitation back into the Southern Hemisphere in austral spring, Figure 7(b) and (c) separate the annual cycle in Figure 7(a) into eastern (55–35 °W) and western (75–55 °W) SAMS regions. Figure 7(b) and (c) show that the progression of the precipitation from the Northern Hemisphere to the Southern Hemisphere is very different in the western and eastern SAMS regions. In particular, over the western SAMS region in austral spring (Figure 7(a)) the precipitation transitions to the Southern Hemisphere more gradually than over the eastern SAMS (Figure 7(b)). Over the eastern SAMS precipitation remains over the warm SSTs in the Northern Hemisphere while a second band of rainfall becomes established quickly near 10–20 °S as the SACZ appears. This analysis suggests that the quick SAMS onset reported in previous studies occurs in the eastern SAMS region but not in the western SAMS region.

The picture that emerges from Figure 7 is in good agreement with the results from the onset date analysis discussed above in connection with Figure 5(a). It suggests the existence of three distinct regional modes of variability that contribute to SAMS onset. Over the western SAMS region (75–55 °W), the precipitation slowly migrates from one hemisphere to the other in a way that more closely resembles the expected migration of the ITCZ over a large near-equatorial landmass. On the other hand, over the eastern SAMS region (55–35 °W), a more complicated pattern of precipitation migration from the Northern Hemisphere to the Southern Hemisphere takes place. In the eastern SAMS region, two distinct patterns of migration are observed, the first one associated with the slow migration of the ITCZ over the Atlantic Ocean (e.g. Hastenrath and Lamb, 1977; Rao and Hada, 1990; Mitchell and Wallace, 1992; Biasutti *et al*., 2004) and the second one likely associated with the quick establishment of the SACZ in the austral spring. The establishment of the SACZ in turn is associated with an abrupt change in the behaviour of frontal systems as they travel through South America (Nieto-Ferreira and Rickenbach, 2010).

These results suggest the presence of important regional differences in the evolution of monsoon onset. In order to explore this issue further an REOF analysis that captures the three regional modes of variability that control ITCZ migration is presented below.

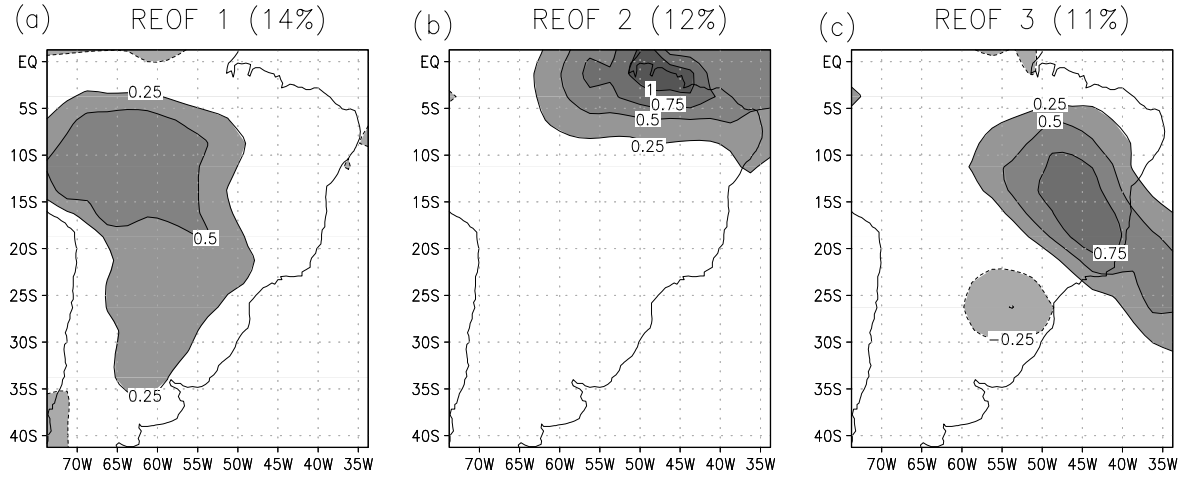

Figure 8. First three rotated EOFs of the GPCP-v2 pentad data from 1979 to 2007 (non-dimensional). (a) REOF1 (14.1% of variance), (b) REOF2 (12.9%) and (c) REOF3 (8.1%).

5. Regional monsoon onset: REOF analysis

An REOF analysis of the 1979–2007 GPCP-v2 pentad dataset at 2.5° horizontal resolution was performed to study the main modes of spatial and temporal variability over South America. The first three REOFs are shown in Figure 8. Figure 9 shows the 29-year averaged principal component (PC) time series annual cycle for the first three modes. In Figure 9 positive values indicate positive rainfall anomalies and vice-versa. The PC time series for the first three REOFs (Figure 9) capture the main features of the annual cycle of rainfall variability over South America.

According to criteria presented in North *et al*. (1982) the first three REOFs in Figure 8 represent three independent modes of variability. Figure 9 shows the 29-year averaged annual cycle of the PC time series for the three first modes. The first REOF (REOF1) explains 14.1% of the variance and shows a coherent pattern of rainfall variability that extends south and southeastward from a maximum over western Amazonia (the region labeled I in Figure 1). The PC time series for REOF1 has a strong annual cycle with negative rainfall anomalies over Amazonia during pentads 23 (April 23–27) through pentad 58 (October 13–17). In contrast to the local monsoon onset definition used in Section 3, the PC time series for each of the three modes of variability described by the REOF analysis allows us to define monsoon onset on a regional basis. This regional monsoon onset criterion is defined here as the time when rainfall anomalies given by the PC time series become positive. Hence based on the time series for PC1 (Figure 9) we determine that pentad 59 (October 18–22) marks the average date of monsoon onset in Amazonia (region I in Figure 1). Table I summarizes the results of the SAMS onset analysis for regions I, II and III (Figure 1) from the rainfall threshold technique, from the REOF analysis and from previous SAMS onset studies. Onset pentads for region I determined using the rainfall threshold (pentad 60) and REOF analyses (pentad 59) are in good agreement with each other and with the multivariate EOF estimate of onset by Silva and Carvalho (2007, SC2007, pentad 61). Gonzalez *et al*. (2007) applied the OLR method of Kousky (1988) to obtain a much earlier onset in the Amazon Basin (pentad 56).

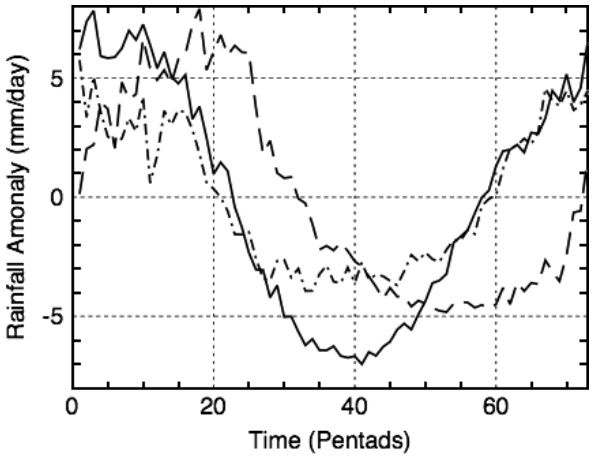

Figure 9. Mean annual time series of the first three principal component time series from the rotated EOF analysis (REOF1 solid, REOF2 dashed and REOF3 dash–dotted).

The annual cycle of rainfall at the mouth of the Amazon (region II in Figure 1) is captured by PC2 and explains 12.9% of the variance. Using the regional monsoon onset definition above, the time series for PC2 (Figure 9) indicates that the monsoon onset over the northeastern SAMS on average occurs on pentad 73 (December 27–31) and therefore about 2 months later than the date of monsoon onset further south, as indicated by the analysis of REOFs 1 and 3. This delayed monsoon onset over northern South America is tied to the slow seasonal migration of the ITCZ rainfall over the tropical Atlantic Ocean (e.g. Hastenrath and Lamb, 1977; Mitchell and Wallace, 1992; Biasutti *et al*., 2004) and is clearly captured by the PC2 time series. This is again in good agreement with the results from the rain threshold technique of onset (Figure 5(a)). The average onset pentad for region II calculated using the rainfall threshold method is pentad 69 (Table I).

A well-known dipole pattern (Nogues-Paegle and Mo, 1997) of rainfall variability with a strong centre in southern Brazil and Uruguay and a second centre of opposite sign anomalies extending southeastward from southeastern Brazil into the Atlantic Ocean is captured in REOF3. This pattern represents variability associated with the SACZ and explains 8.1% of the variance. In fact, Figure 9 shows that PC3 captures the annual cycle of SACZ rainfall showing that the SACZ (region III in Figure 1) becomes established on average at around pentad 61 (October 28–November 1) and dissipates by the following March when the rainfall maximum returns to the southern side of the dipole located over Uruguay and southern Brazil (region IV in Figure 1). A comparison between the PC time series for REOF1 and REOF3 suggests that the SACZ becomes established on average two pentads after monsoon onset occurs on the western part of the SAMS. This suggests that the onset of the monsoon over the western part of the SAMS produces the right dynamical conditions for the establishment of the SACZ. This hypothesis is further investigated in a companion study (Nieto-Ferreira and Rickenbach, 2010).

The general characteristics of the progression of monsoon onset gleaned from the regional onset analysis in this section and from the local onset analysis in Section 3 are in good agreement. However, a slight modification to the interpretation of the results in Section 3 is suggested by the REOF analysis. The picture of onset suggested by the local onset analysis in Section 3 (and also from previous studies) was that onset begins in the subtropical southeast progressing northward and in the tropical northwest progressing southeastward with the two patterns converging to fill most of the SAMS by late October to early November. The REOF analysis instead shows that in the subtropical SAMS, rainfall progresses northeastward from Uruguay/southern Brazil to southeastern Brazil as the SACZ becomes established.

In summary, the first three modes of the REOF analysis are in agreement with the idea that three main regional modes of variability participate in the onset of the South American monsoon. This result provides the basis for a new three-stage conceptual model of monsoon onset, summarized below in the conclusions.

6. Conclusions

This study builds on previous studies of monsoon onset definition, timing and regional variability to construct a new integrated picture of monsoon onset and proposes a three-stage conceptual model of monsoon onset in South America. This analysis is unique in the sense that it is based on the GPCP-v2 pentad precipitation dataset, a product that is well-suited for studying monsoon onset across tropical and subtropical South America because of its uniform temporal and spatial coverage. The approach used in this study has been two-pronged, combining results from a local monsoon onset definition based on a rainfall threshold criterion with a regional monsoon onset definition based on an REOF analysis. This novel combined approach was useful to identify regions of South America that show contrasting seasonal cycles of rainfall variability and likely have distinct onset mechanisms. The general characteristics of the progression of monsoon onset in South America gleaned from this analysis are in good agreement with previous studies.

A slightly modified version of the Marengo *et al.* (2001) monsoon onset definition was applied to the GPCP-v2 pentad precipitation data over the entire SAMS region. This rainfall threshold analysis shows that the onset of the SAMS begins in late September over northwestern Amazonia and slowly progresses southeastward. A second monsoon onset pattern that begins in the subtropics in mid-September and progresses northwestward is also present. The two onset patterns appear to converge and fill most of the SAMS domain with monsoonal rains by early December. At the mouth of the Amazon River and in northeastern Brazil onset occurs later in early-to-mid December and late December to late January, respectively. Regions where the onset criterion is seldom or never met are also discussed, notably near equatorial regions where it rains year-round and in parts of subtropical South America where transient systems bring rainfall year-round. On interannual timescales, this study confirms that SAMS onset is influenced by ENSO. In particular, during El Niño years monsoon onset tends to occur later than usual across the SAMS region. On the other hand, during La Niña episodes the tendency for early monsoon onset dates in the 5°N–5°S portion of the SAMS domain contrasts with the mix of early and late monsoon onset dates elsewhere in the SAMS domain.

While previous studies have suggested that SAMS onset seems to occur quickly, a zonal averaged analysis presented in this study shows that onset is gradual in the western SAMS region (to the west of 60°W) with fast onset occurring only in the SACZ region. Moreover, a regional monsoon onset analysis based on REOFs indicates that the SACZ is established only after monsoon onset has occurred over the western SAMS suggesting that this region plays a role in producing the right dynamical conditions to trigger monsoon onset in the SACZ region.

The results from this combined local and regional monsoon onset analysis are used to propose a three-stage conceptual model of SAMS onset. The first stage of onset begins in late September in the tropical northwest portion of the SAMS region and slowly progresses southeastward following the gradual migration of the sun into the Southern Hemisphere. The second stage of monsoon onset is marked by a quick shift of rainfall from Uruguay/southern Brazil to southeastern Brazil. This stage of monsoon onset is associated with the establishment of the SACZ. The third stage of SAMS onset occurs in late December when Atlantic ITCZ rainfall finally arrives at the northern coast of Brazil after the Atlantic cold tongue dissipates.

This study sets the stage for two companion studies (in preparation), on the mechanisms for SAMS monsoon

onset. The first is an analysis of detailed observations of precipitating cloud systems from the TRMM satellite to study regional changes in the organization and structure of convection as the monsoon begins and to help further our understanding of the mechanisms for monsoon onset in tropical and subtropical South America. The second study addresses the possible role of western SAMS rainfall forcing in producing the shift in dynamical conditions that leads to monsoon onset in the SACZ region and the role of cold fronts in SAMS monsoon onset (Nieto-Ferreira and Rickenbach, 2010).

Acknowledgements

This study has been funded by a grant (Award Number: NA07OAR4310495) from the National Oceanic and Atmospheric Administration Climate and Global Change Program Climate Prediction Program for the Americas (NOAA-CPPA). The authors would like to thank two anonymous reviewers for their valuable comments.

References

Adler RF and coauthors. 2003. The version-2 Global Precipitation Climatology Project (GPCP-V2) monthly precipitation analysis (1979-present). *Journal of Hydrometeorology* **4**: 1147–1167.

Biasutti M, Battisti DS, Sarachik ES. 2004. Mechanisms controlling the annual cycle of precipitation in the tropical Atlantic sector in an atmospheric GCM. *Journal of Climate* **17**: 4708–4723.

Chang CP, Chen GTJ. 1995. Tropical circulation associated with southwest monsoon onset and westerly surges over the South China Sea. *Monthly Weather Review* **123**: 181–196.

Fortune M, Kousky V. 1983. Two severe freezes in Brazil: precursors and synoptic evolution. *Monthly Weather Review* **111**: 181–196.

Fu R, Li W. 2004. The influence of the land surface on the transition from dry to wet season in Amazonia. *Theoretical and Applied Climatology* **78**: 97–110.

Gan MA, Kousky VE, Ropelewski CF. 2004. The South America monsoon circulation and its relationship to rainfall over West Central Brazil. *Journal of Climate* **17**: 47–66.

Gan MA, Moscati MCL. 2003. Estação chuvosa de 2001/02 na região Centro-Oeste do Brasil – 2001/02 rainy season in West-Central Brazil. *Rev. Bras. Meteor.* **18-2**: 181–194.

Gan MA, Rao VB, Moscati MCL. 2006. South American monsoon indices. *Atmospheric Science Letters* **6**: 219–223.

Gandu AW, Geisler JE. 1991. A primitive equations model study of the effect of topography on the summer circulation over tropical South America. *Journal of the Atmospheric Sciences* **48**: 1822–1836.

Garcia S, Kayano MT. 2009. Determination of the onset dates of the rainy season in central Amazon with equatorially antisymmetric outgoing longwave radiation. *Theoretical and Applied Climatology* **97**: 361–372, DOI 10.1007/s00704-008-0080-y.

Garreaud RD. 2000. Cold air intrusions over subtropical South America: structure and dynamics. *Monthly Weather Review* **128**: 2544–2599.

Gonzalez M, Vera C, Liebmann B, Marengo J, Kousky V, Allured D. 2007. The nature of the rainfall onset over central South America. *Atmósfera* **20**: 377–394.

Hastenrath S, Greischar L. 1993. Further work on the prediction of northeast Brazil rainfall anomalies. *Journal of Climate* **6**: 743–758.

Hastenrath S, Lamb P. 1977. *Climatic Atlas of the Tropical Atlantic and Eastern Pacific Oceans*. University of Wisconsin Press: Madison; 112 pp.

Horel JD, Hahmann AN, Geisler JE. 1989. An investigation of the annual cycle of convective activity over the tropical Americas. *Journal of Climate* **2**: 1388–1403.

Jones C, Carvalho LMV. 2002. Active and break phases in the South American monsoon system. *Journal of Climate* **15**: 905–914.

Kousky VE. 1985. Atmospheric circulation changes associated with rainfall anomalies over Tropical Brazil. *Monthly Weather Review* **113**: 1951–1957.

Kousky VE. 1988. Pentad outgoing longwave radiation climatology for the South American sector. *Rev. Bras. Meteor.* **3**: 217–231.

Lenters JD, Cook K. 1995. Simulation and diagnosis of the regional summertime precipitation climatology of South America. *Journal of Climate* **8**: 2988–3005.

Li W, Fu R. 2004. Transition of the large-scale atmospheric and land surface conditions from the dry to the wet season over Amazonia as diagnosed by the ECMWF re-analysis. *Journal of Climate* **17**: 2637–2651.

Li W, Fu R. 2006. Influence of cold air intrusions on the wet season onset over Amazonia. *Journal of Climate* **19**: 257–275.

Liebmann B, Kiladis GN, Marengo JA, Ambrizzi T, Glick JD. 1999. Submonthly convective variability over South America and the South Atlantic Convergence zone. *Journal of Climate* **12**: 1877–1891.

Liebmann B, Marengo JA. 2001. Interannual variability of the rainy season and rainfall in the Brazilian Amazon Basin. *Journal of Climate* **14**: 4308–4318.

Lindzen RS, Nigam S. 1987. On the role of sea surface temperature gradients in forcing low level winds and convergence in the tropics. *Journal of the Atmospheric Sciences* **44**: 2418–2436.

Machado LAT, Laurent H, Dessay N, Miranda I. 2004. Seasonal and diurnal variability of convection over the Amazonia: a comparison of different vegetation types and large scale forcing. *Theoretical and Applied Climatology* **78**: 61–77.

Marengo JA, Liebmann B, Kousky VE, Filizola NP, Wainer I. 2001. Onset and end of the rainy season in the Brazilian Amazon Basin. *Journal of Climate* **14**: 833–852.

Mitchell TP, Wallace JM. 1992. The annual cycle in equatorial convection and sea surface temperature. *Journal of Climate* **5**: 1140–1156.

Moura AD, Shukla J. 1981. On the dynamics of droughts in Northeast Brazil: observations, theory and numerical experiments with a general circulation model. *Journal of the Atmospheric Sciences* **38**: 2653–2675.

Nieto-Ferreira R, Rickenbach TM. 2010. The role of cold fronts in the onset of the South American monsoon. Submitted to the *Quarterly Journal of Royal Meteorological Society* (in press).

Nogues-Paegle JN, Mo KC. 1997. Alternating wet and dry conditions over South America during summer. *Monthly Weather Review* **125**: 279–291.

North GR, Bell TL, Cahalan RF, Moeng FJ. 1982. Sampling errors in the estimation of empirical orthogonal functions. *Monthly Weather Review* **110**: 699–706.

Raia A, Cavalcanti IF. 2008. The life cycle of the South American monsoon system. *Journal of Climate* **21**: 6227.

Rao VB, Hada K. 1990. Characteristics of rainfall over Brazil: annual variations and connections with the southern oscillation. *Theoretical and Applied Climatology* **42**: 81–91.

Rickenbach TM, Nieto-Ferreira R, Halverson J, Herdies D, Silva Dias MAF. 2002. Modulation of convection in the Southwestern Amazon Basin by extratropical stationary fronts. *Journal of Geophysical Research* **107**(D20): 8040, DOI: 10.1029/2000JD000263.

Rickenbach TM, Nieto-Ferreira R, Rickenbach J, Wright E. 2009. Monsoon in the Americas: opportunities and challenges. *Geography Compass* **3**: 1–16, DOI: 10.1111/j.1749–8198.2009.00266.x.

Silva AE, Carvalho LMV. 2007. Large-scale index for South America Monsoon (LISAM). *Atmospheric Science Letters* **8**: 51–57, DOI: 10.1002/asl.150.

Thorncroft CD, Hoskins BJ, McIntyre ME. 1993. Two paradigms of baroclinic wave life-cycle behavior. *Quarterly Journal of Royal Meteorological Society* **119**: 17–55.

Velasco I, Fritsch J. 1987. Mesoscale convective complexes in the Americas. *Journal of Geophysical Research* **92**: 9591–9613.

Vera CS, Vigliarolo PK. 2000. A diagnostic study of cold-air outbreaks over South America. *Monthly Weather Review* **128**: 3–24.

Wang H, Fu R. 2002. Cross-equatorial flow and seasonal cycle of precipitation over South America. *Journal of Climate* **15**: 1591–1608.

Zeng N, Yoon J-H, Marengo JA, Subramanian A, Nobre CA, Mariotti A, Neelin DJ. 2008. Causes and impacts of the 2005 Amazon drought. *Environmental Research Letters* **3**: 014002, DOI: 10.1088/1748-9326/3/1/014002, 9pp.

Zhou J, Lau KM. 1998. Does a monsoon climate exist over South America?. *Journal of Climate* **11**: 1020–1040.

Zhou J, Lau W-K. 2001. Principal modes of interannual and decadal variability of summer rainfall over South America. *International Journal of Climatology* **21**: 1623–1644.

